

Article

Optimal Scheduling of Virtual Power Plant with Flexibility Margin Considering Demand Response and Uncertainties

Yetuo Tan ¹, Yongming Zhi ², Zhengbin Luo ³, Honggang Fan ^{4,*}, Jun Wan ⁵ and Tao Zhang ⁶¹ Jiangxi Port Group Co., Ltd., Nanchang 332000, China² China Water Resources Pearl River Planning, Surveying and Designing Co., Ltd., Guangzhou 510610, China³ Jiangxi Transportation Institute Co., Ltd., Nanchang 330200, China⁴ State Key Laboratory of Hydrosience and Engineering, Department of Energy and Power Engineering, Tsinghua University, Beijing 100084, China⁵ Jiangxi Jiepai Navigation and Electricity Hub Management Office, Yingtan 335000, China⁶ Department of Electrical Engineering, Tsinghua University, Beijing 100084, China

* Correspondence: fanhonggang@tsinghua.org.cn

Abstract: The emission reduction of global greenhouse gases is one of the key steps towards sustainable development. Demand response utilizes the resources of the demand side as an alternative of power supply which is very important for the power network balance, and the virtual power plant (VPP) could overcome barriers to participate in the electricity market. In this paper, the optimal scheduling of a VPP with a flexibility margin considering demand response and uncertainties is proposed. Compared with a conventional power plant, the cost models of VPPs considering the impact of uncertainty and the operation constraints considering demand response and flexibility margin characteristics are constructed. The orderly charging and discharging strategy for electric vehicles considering user demands and interests is introduced in the demand response. The research results show that the method can reduce the charging cost for users participating in reverse power supply using a VPP. The optimizing strategy could prevent overload, complete load transfer, and realize peak shifting and valley filling, solving the problems of the new peak caused by disorderly power utilization.



Citation: Tan, Y.; Zhi, Y.; Luo, Z.; Fan, H.; Wan, J.; Zhang, T. Optimal Scheduling of Virtual Power Plant with Flexibility Margin Considering Demand Response and Uncertainties. *Energies* **2023**, *16*, 5833. <https://doi.org/10.3390/en16155833>

Academic Editor: Javier Muñoz Antón

Received: 5 May 2023

Revised: 13 July 2023

Accepted: 28 July 2023

Published: 7 August 2023



Copyright: © 2023 by the authors. Licensee MDPI, Basel, Switzerland. This article is an open access article distributed under the terms and conditions of the Creative Commons Attribution (CC BY) license (<https://creativecommons.org/licenses/by/4.0/>).

Keywords: virtual power plant (VPP); flexibility margin; demand response; uncertainties; integrated energy system; renewable energy

1. Introduction

With the increasing energy crisis and pollution problems, new technologies such as the smart grid, energy internet, energy hub, integrated energy system (IES), and virtual power plant (VPP) have been introduced to realize the multi-energy coordinated supply and cascade utilization of energy [1,2]. Meanwhile, a high proportion of wind power and photovoltaic power generation are connected to the power grid, resulting in a large increase in flexibility demands [3]. The traditional scheduling strategy relies on the improvement of a rotating reserve capacity to ensure the stable operation of a power system which is unable to cope with the rapidity of net load changes. Therefore, demand responses and flexibility loads have gradually become one of the research hotspots of current power system optimization scheduling. Moreover, the concept of a virtual power plant was proposed to integrate different energy resources such as distributed generations, energy storage systems, and flexibility loads to provide system support services [4,5].

A VPP benefits from the electricity market or dynamic pricing to shift energy demand [6–8]. A VPP always focuses on economic benefits and the optimization of VPP operation is closely related to it. Many researchers have conducted a lot of research on it and have also achieved many excellent results. The scheduling optimization of VPPs usually aims to minimize operating costs and maximize operating benefits. Moreover, a

lot of papers focus on multiple objectives such as cost, benefits, and power grid stability through methods such as the fuzzy multi-objective method [9]. The currently used optimal algorithms include the linear optimization algorithm [10], mixed integer linear programming algorithm [11,12], hierarchical optimization algorithm [13], differential evolution algorithm [14], adaptive heuristic algorithm [15,16], and robust optimization algorithm [17]. Li et al. analyzed the feasibility of VPPs by means of local renewable energy plant construction and the updating of high-efficiency appliances located at electricity customers [18]. Some scholars use the data envelopment analysis method to consider the comprehensive efficiency of the candidate units for economy, environmental protection, stability, and reliability, and they select the units to build a VPP according to the results [19]. Sousa et al. proposed a simulated annealing approach to address energy resource management from the point of view of a VPP, and the results showed that a VPP can purchase additional energy from a set of external suppliers [20].

The VPPs aggregate a lot of equipment which include wind power, photovoltaic power (PV), electric boilers, air conditioners, electric vehicles, flexibility loads, and so on [21–23]. Moreover, the uncertainties of renewable energy output, energy demand, and market price bring a huge challenge to the optimal scheduling of VPPs [24,25]. The uncertainty of renewable energy output mainly includes wind and photovoltaic power. The uncertainty of wind power output is mainly due to the randomness of wind speed, and the uncertainty of photovoltaic power output is mainly due to solar radiation. Moreover, the weather can affect renewable energy output, especially on a rainy day. Energy demands are uncertainty in VPP optimization problems which derive from prediction and measurement errors. The uncertainties of market price include electricity price, natural gas price, and heating price which have very strong fluctuations. A lot of optimization approaches considering uncertainty have been studied by different scholars. These include the Monte Carlo simulation [26,27], robust optimization [28], rolling horizon, stochastic dominance [29], fuzzy chance constraint programming constraints [30], and point estimation methods [31]. Some scholars focused on the fluctuation problem of VPP output. Hooshmand et al. [32] introduced the user side of power stations in a virtual power plant and built a double-layer model to increase revenues and to provide backup service to the energy system.

Previous research has already studied the optimization of VPP operation and achieved a lot of results. However, some studies only considered the uncertainty of wind power and PV, and the method could only handle the constraint conditions without stochastic variables. In this paper, a flexibility margin considering demand response and uncertainties is analyzed with a stochastic chance constrained planning method. Moreover, the demand response of electric vehicles and traditional loads are optimized to guide customers' power consumption behavior.

This paper is structured as follows: Section 2 describes an overview of the VPP's structure, which includes the model formulation, constraint conditions, and objective function. Section 3 describes the flexibility margin considering demand response. Section 4 gives an example to analyze the VPP. Section 5 concludes this research study by describing challenges and future work.

2. VPP Structure

As shown in Figure 1, the VPP consists of a distributed photovoltaic system, combined heat and power system, gas-fired boiler, absorption refrigeration unit, refrigeration unit, electric boiler, electric vehicle, cooling storage, electric storage, thermal storage, electrical load, cooling load, heating load, electricity market, and so on. The VPP operator is obligated to satisfy the demands of consumers by purchasing energy from the electricity market. In the electricity market, the VPP operator allows consumers to participate in the market to alleviate supply pressure, inducing load reductions by incentivizing consumers. Moreover, the VPP serves as a backup that shifts loads from peak to off-peak periods.

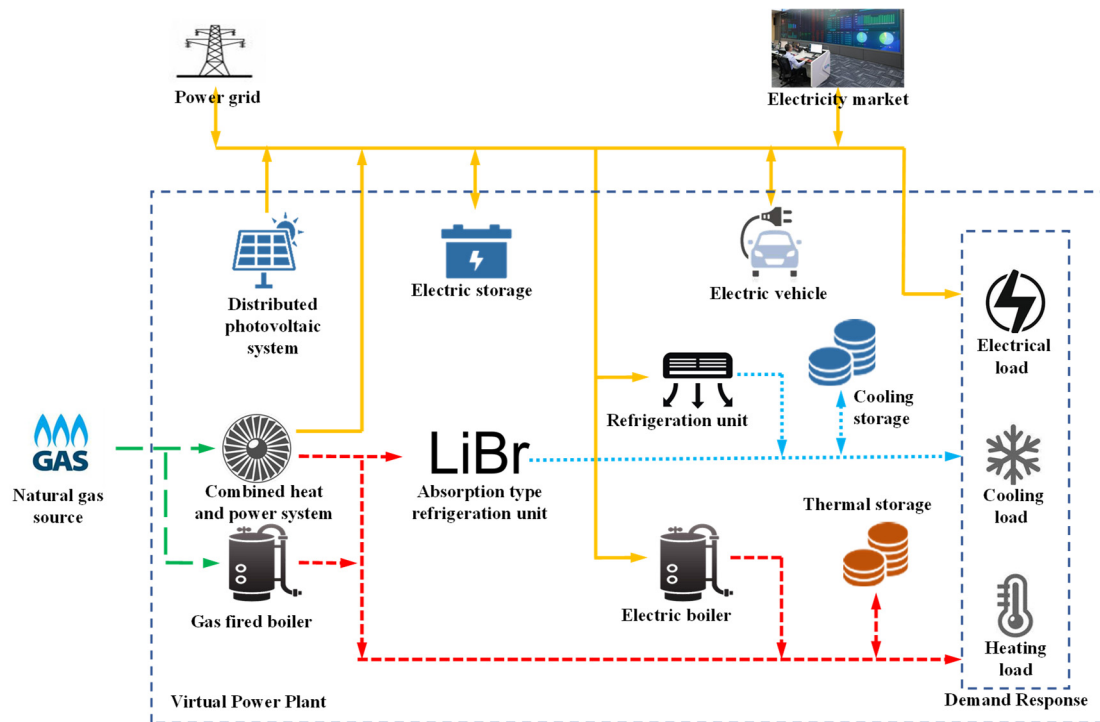


Figure 1. Basic structure of VPP.

2.1. Model Formulation of the VPP

2.1.1. Distributed Photovoltaic System

The power output of the distributed photovoltaic system is greatly affected by environmental factors. The power output is determined by light intensity and ambient temperature in an ideal situation which is shown as follows:

$$P_{PV} = f_{pv} P_{PVR} \frac{G}{G_S} [1 + \alpha_{PV}(T - T_S)] \quad (1)$$

where P_{PV} represents the power output of the photovoltaic power system, MW. f_{pv} and P_{PVR} represent the reduction coefficient and rated power output in the standard state. G and G_S represent the illumination intensity of the current position and the standard state. α_{PV} is the power temperature reduction coefficient in the standard state. T and T_S represent the temperature on the surface of the photovoltaic panel and the temperature of the photovoltaic surface in the standard state.

2.1.2. Combined Heat and Power System

The combined heat and power (CHP) system generates electricity and heating energy by burning natural gas. Collecting the heating energy could improve the energy utilization rate of the gas turbine field in the CHP. Moreover, the output of heating and power energy are proportional to the consumption of natural gas. The calculation formulas are as follows:

$$P_{EGT} = \eta_E F_{GT} \quad (2)$$

$$P_{HGT} = \eta_H F_{GT} \quad (3)$$

$$\eta_E + \eta_H + \eta_{loss} = 1 \quad (4)$$

where P_{EGT} and P_{HGT} are the electric power output and thermal power output by the CHP, MW. η_E , η_H , η_{loss} indicate the electric efficiency, thermal efficiency, and heat loss rate of the CHP, respectively. F_{GT} represents the energy of gas combustion.

2.1.3. Gas-Fired Boiler

The gas-fired boiler consumes natural gas to produce thermal power which meets thermal balance. The thermal output of the gas boiler is proportional to the natural gas consumption, which is as follows:

$$P_{GB} = \eta_{GB} F_{GB} \quad (5)$$

where P_{GB} is the thermal output power of the gas boiler. η_{GB} indicates the gas utilization efficiency of the gas boiler. F_{GB} is the consumption of natural gas.

2.1.4. Refrigeration Unit

The electric refrigeration unit could supply cooling to the consumer, and the output of the refrigerator is proportional to the input electric power which is as follows:

$$P_{CEC} = \eta_{EC} P_{EC} \quad (6)$$

where P_{EC} is the cooling output of the electric refrigeration unit. η_{EC} indicates the utilization efficiency of the electric refrigeration unit.

The absorption refrigeration unit utilizes the working medium to release cooling. The cooling output is directly proportional to the input thermal power and electric power, which are as follows:

$$P_{HRC} = \eta_{RC} P_{RC} \quad (7)$$

where P_{HRC} and P_{RC} are the cooling output and heating input of the absorption refrigeration unit. η_{RC} is the refrigeration efficiency.

2.1.4.1. Energy Storage Unit

The VPP includes electric, heating, and cooling storage units, which meet the loads' demands. The energy storage unit has the function of balancing peaks and valleys which could improve the coefficient of energy utilization. The mathematical models are as follows:

$$E_{ES}(t) = (1 - \eta_{ES})E_{ES}(t - 1) + (P_{ESC}\eta_{ESC} - P_{ESD}/\eta_{ESD})\Delta t \quad (8)$$

$$\alpha_{ESC} + \alpha_{ESD} \leq 1 \quad (9)$$

$$0 \leq P_{ESC} \leq \alpha_{ESC} P_{ESC \max} \quad (10)$$

$$0 \leq P_{ESD} \leq \alpha_{ESD} P_{ESD \max} \quad (11)$$

$$E_{ES \min} \leq E_{ES}(t) \leq E_{ES \max} \quad (12)$$

where $E_{ES}(t)$ and $E_{ES}(t - 1)$ represent the electric energy stored by the electric energy storage unit at time t and time $t - 1$. P_{ESC} and P_{ESD} are the charging power and discharge power. η_{ES} , η_{ESC} , η_{ESD} are the self-discharge ratio, charging efficiency, and discharge efficiency, respectively. $P_{ESC \max}$ and $P_{ESD \max}$ are the rated charging power and the rated discharge power, respectively. $E_{ES \min}$ and $E_{ES \max}$ are the lower and upper climbing limits.

Moreover, Heating exchanges of thermal storage unit are as follows:

$$Q_{TS}(t) = (1 - \eta_{TS})Q_{TS}(t - 1) + (P_{TSC}\eta_{TSC} - P_{TSD}/\eta_{TSD})\Delta t \quad (13)$$

$$\alpha_{TSC} + \alpha_{TSD} \leq 1 \quad (14)$$

$$0 \leq P_{TSC} \leq \alpha_{TSC} P_{TSC \max} \quad (15)$$

$$0 \leq P_{TSD} \leq \alpha_{TSD} P_{TSD \max} \quad (16)$$

$$Q_{TS \min} \leq Q_{TS}(t) \leq Q_{TS \max} \quad (17)$$

where $Q_{TS}(t)$ and $Q_{TS}(t-1)$ represent the thermal stored by thermal storage unit at time t and time $t-1$. $Q_{TS}(t)$ and $Q_{TS}(t-1)$ are the charging heating and discharge heating at time t and time $t-1$. $\eta_{TS}, \eta_{TSC}, \eta_{TSD}$ are the self-discharge ratio, charging efficiency and discharge efficiency, respectively. $P_{TSC\ max}$ and $P_{TSD\ max}$ are the rated charging thermal and the rated discharge thermal, respectively. $E_{ES\ min}$ and $E_{ES\ max}$ are the lower and upper climbing limits.

2.2. Objective Function

The VPP was modelled using the mixed integer linear programming (MILP) method in LINGO software. The objective of the optimization was to maximize the VPP profit, which consists of the incomes of participating power and gas markets, benefits from demand sides, carbon emission fees, and unbalanced penalties. Therefore, the objective function is defined as follows:

$$\begin{aligned} \max C_m = & \sum_{t=1}^T c_d(t)P_d(t) - \sum_{t=1}^T F_{carbon}(t)\eta_{carbon} + \sum_{t=1}^T c_l(t)P_l(t) - \\ & \sum_{t=1}^T F_{eco}(t)P_{c,a}(t) - c_{co}(t) \sum_{t=1}^T P_{TS}(t) - C_b \end{aligned} \quad (18)$$

where $c_d(t)$ is the prices in the electricity market. η_{carbon} is the fee of carbon emissions, yuan/t CO₂. $c_l(t)$ is the price for VPP's users. $C_{co}(t)$ is the fee of energy storage loss and C_b is the unbalanced penalty cost.

The operating cost is the sum of the purchased energy cost and equipment maintenance cost which are showed as follows:

$$F_{eco} = C_{op} + C_{en} \quad (19)$$

where F_{eco} is the operation cost. C_{op} is the maintenance cost. C_{en} is the purchased energy cost which is shown as follows:

$$C_{op} = \sum_{t=1}^T [\lambda_{WT}P_{WT}(t) + \lambda_{PV}P_{PV}(t) + \lambda_{GT}P_{GT}(t) + \lambda_{GB}P_{GB}(t) + \lambda_{EC}P_{EC}(t) + \lambda_{RC}P_{RC}(t) + \lambda_{ES}P_{ES}(t) + \lambda_{TS}P_{TS}(t)]\Delta t \quad (20)$$

$$C_{en} = \delta_{gas} \sum_{t=1}^T [F_{GT}(t) + F_{GB}(t)]\Delta t + \delta_{el} \sum_{t=1}^T P_{grid}(t)\Delta t \quad (21)$$

where $P_X(t)$ represents the average power output of X. λ_X represents the cost coefficient of operation and maintenance. δ_{gas} and δ_{el} are the prices of natural gas and electricity, respectively. $F_{GT}(t), F_{GB}(t), P_{grid}(t)$ indicate the average combustion ratio of natural gas in CHP, the average combustion ratio of natural gas in the gas boiler, and the average input of the power grid, respectively.

The carbon emissions of a VPP could be calculated using the following equation:

$$F_{carbon} = \sum_{t=1}^T \{\lambda_{gas}[F_{GB}(t) + F_{GT}(t)] + \lambda_{el}P_{grid}(t)\}\Delta t \quad (22)$$

where F_{carbon} represents the carbon emissions of the VPP, t CO₂. $\lambda_{gas}, \lambda_{el}$ are the carbon emission coefficients of natural gas and the power grid, t CO₂/MW.

2.3. Constraint Conditions

In order to make the energy network safe and stable, the variables in the energy network need to meet certain constraints in the VPP. The energy conservation constraints include

$$P_{grid} + P_{WT} + P_{PV} + P_{EGT} = P_E + P_{EC} + P_{ESC}(-P_{ESD}) \quad (23)$$

$$P_{HGT} + P_{GB} = P_H + P_{RC} + P_{TSC}(-P_{TSD}) \quad (24)$$

$$\eta_{EC}P_{EC} + \eta_{RC}P_{RC} = P_C \quad (25)$$

where P_{grid} is the power supply of the power grid. P_E, P_H, P_C are the electric load, thermal load, and cooling load.

All equipment operates between the maximum output and the minimum output to ensure long-term safe operation in VPP. The constraints include

$$0 \leq P_{GT} \leq P_{GT \max} \quad (26)$$

$$0 \leq P_{GB} \leq P_{GB \max} \quad (27)$$

$$0 \leq P_{CEC} \leq P_{CEC \max} \quad (28)$$

$$0 \leq P_{HRC} \leq P_{HRC \max} \quad (29)$$

$$0 \leq P_{grid} \leq P_{grid \max} \quad (30)$$

$$0 \leq F_{GB} + F_{GT} \leq F_{max} \quad (31)$$

where $P_{GT \max}, P_{GB \max}, P_{CEC \max}, P_{HRC \max}$ are the maximum output of the CHP, gas boiler, and refrigeration unit. $P_{grid \max}$ and F_{max} represent the maximum electric power supplied by the power grid and the maximum ratio of natural gas supplied by the natural gas pipeline.

The energy storage unit constraints include electric, heating, and cooling storage balance constraints which are as follows:

$$E_{ES}(t) = (1 - \eta_{ES})E_{ES}(t - 1) + (P_{ESC}\eta_{ESC} - P_{ESD}/\eta_{ESD})\Delta t \quad (32)$$

$$\alpha_{ESC} + \alpha_{ESD} \leq 1 \quad (33)$$

$$0 \leq P_{ESC} \leq \alpha_{ESC}P_{ESC \max} \quad (34)$$

$$0 \leq P_{ESD} \leq \alpha_{ESD}P_{ESD \max} \quad (35)$$

$$E_{ES \min} \leq E_{ES}(t) \leq E_{ES \max} \quad (36)$$

$$Q_{TS}(t) = (1 - \eta_{TS})Q_{TS}(t - 1) + (P_{TSC}\eta_{TSC} - P_{TSD}/\eta_{TSD})\Delta t \quad (37)$$

$$\alpha_{TSC} + \alpha_{TSD} \leq 1 \quad (38)$$

$$0 \leq P_{TSC} \leq \alpha_{TSC}P_{TSC \max} \quad (39)$$

$$0 \leq P_{TSD} \leq \alpha_{TSD}P_{TSD \max} \quad (40)$$

$$Q_{TS \min} \leq Q_{TS}(t) \leq Q_{TS \max} \quad (41)$$

where $\alpha_{ESC}, \alpha_{ESD}, \alpha_{TSC}, \alpha_{TSD}$ are binary parameters (0–1) which could constrain the energy storage unit so that it could not charge and discharge simultaneously.

3. Flexibility Margin Considering Demand Response

Terminal customers are a strong uncertainty, and the load could be divided into the interruptible, adjustable, and sensitive loads [15,33,34]. We have divided the load demand into certainty and uncertainty loads. The certainty load means the invariable load which must be supplied, and the uncertainty loads are variable loads in the flexibility margin. According to the theory of uncertainty, the electricity price is described by the probability distribution. The output of renewable energy is analyzed by weather prediction.

3.1. Flexibility Margin

The flexibility of the VPP refers to the degree of balance between the supply and demand of energy. The difference between the power load and the output of photovoltaic power is described as the net load. We can describe the VPP flexibility requirement as being calculated by

$$F_t = P_{netload,t+1} - P_{netload,t} \quad (42)$$

$$P_{netload,t} = P_{load,t} - P_{PV,t} \quad (43)$$

$$\begin{aligned} F_t^{up} &= \{F_t | F_t > 0\} \\ F_t^{down} &= \{F_t | F_t < 0\} \end{aligned} \quad (44)$$

where $P_{PV,t}$ is the actual output of photovoltaic power generation at time t . F_t^{up} , F_t^{down} are the upward and downward flexibility requirements at time t . $P_{netload,t}$, $P_{load,t}$ are the power load and net load at time t . $P_{netload,t+1}$ is the net load at time $t + 1$. Moreover, the prediction error of the photovoltaic system output satisfied the normal distribution, which is described as $\Delta P_{PV,t} \sim N(0, \sigma_{PV,t})$.

3.2. Flexibility Indicators

The flexibility margin is described as the difference between flexible supply and demand. The direction includes up and down.

$$\begin{cases} F_{ru_up} = F_{gong,t}^{up} - F_t^{up} \\ F_{ru_down} = F_{gong,t}^{down} - F_t^{down} \end{cases} \quad (45)$$

where F_{ru_up} , F_{ru_down} are the upward and downward flexibility margins, respectively.

4. Example Analysis

There is a community which has the data showing electricity load, cooling load, heating load, light radiation, and temperature in Beijing. The time scale is one hour. The charging price of electric vehicles refers to the charging standard of Beijing electric vehicles. The valley periods are 23:00–7:00, the usual periods are 8:00–10:00, 16:00–18:00, and 22:00, and the peak periods are 11:00–15:00 and 19:00–21:00, which are shown in Table 1. The electricity price of users is shown in Table 2. The valley periods are 23:00–6:00, 7:00–9:00, 12:00–18:00, 10:00–11:00–11:00, and 19:00–22:00, and the selling price of energy storage equipment to the grid is set at 0.45 yuan/kWh, which is higher than the electricity price of both valleys and lower than the usual price of both.

Table 1. Charging price of the electric vehicles.

Times	Prices (yuan/kWh)
valley period	0.3946
usual period	0.685
peak period	1.0044

Table 2. Purchase electricity price of users.

Times	Prices (yuan/kWh)
valley period	0.284
usual period	0.52
peak period	0.89

Moreover, the carbon emission of the CHP unit is 0.798 t/(MWh), and the carbon trading price is 52.78 yuan/t. The peak power load of the user is 150 kW, the peak cooling load is 201 kW, the peak heating load is 672 kW, and the PV installation capacity is within

the range of 0.5~2 times of the power capacity. Considering the charging demand of electric vehicles, the installed capacity of the battery is 4000 Ah, the installed capacity of air conditioning is 220 kW, the installed capacity of ice storage equipment is 500 kWh, the installed capacity of the electric boiler is 70 kW, and the installed capacity of heat storage tank equipment is 120 kWh. The cost parameters of the energy unit are shown in Table 3.

Table 3. The cost parameters of the energy unit.

Technical Equipment	Installation Cost yuan/kW	Running Costs yuan/kWh	Efficiency		Period (Year)
			Electrical Efficiency	Heating Efficiency	
Internal combustion engine	5000	0.072	0.4	0.45	30
Photovoltaic system	7500	0.01	0.12	0	25
Energy storage system	4000	0.0022		0.81	15

In our model, the prices of different energies are shown in Figure 2. The gas price and photovoltaic feed-in tariff do not change with time. However, the electricity prices in different voltages change at different times. Moreover, the charging load of the electric vehicle benchmark is shown in Figure 3. It changes with a normal distribution.

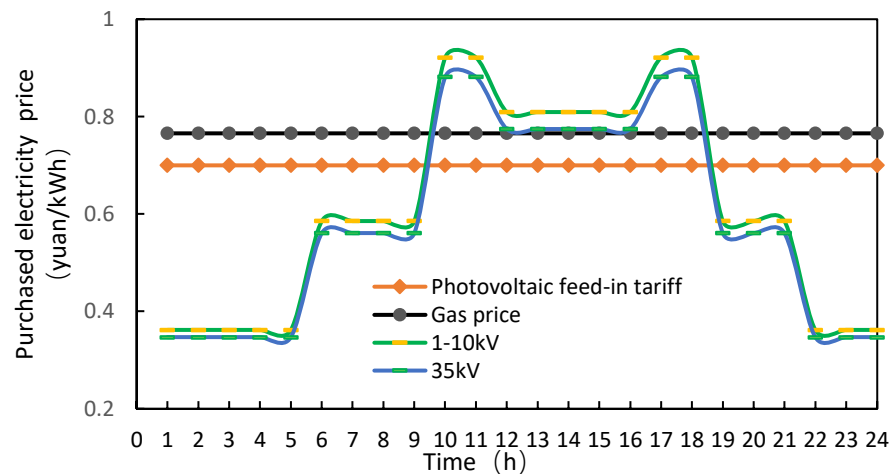


Figure 2. Prices of different energy.

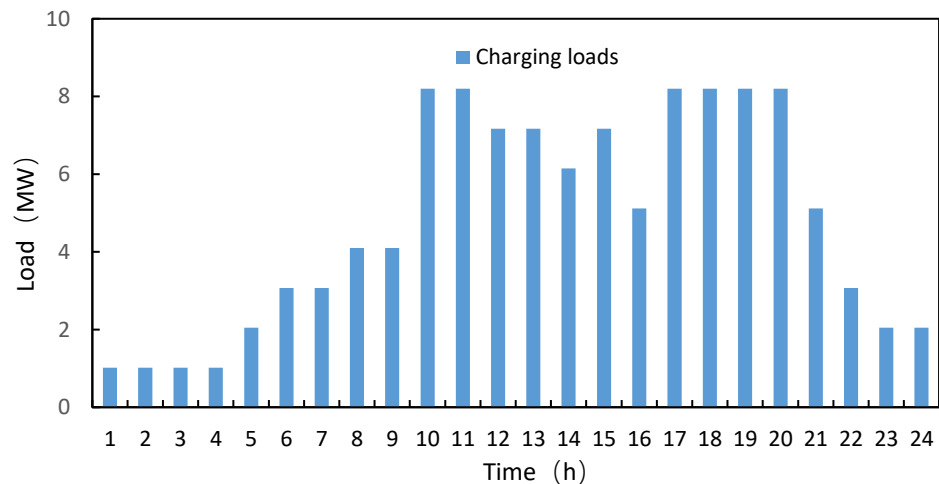


Figure 3. Charging load of electric vehicle benchmark.

The typical daily operation is shown in the following figure which is the power balance in the traditional model without a VPP. At the low price, the charging station buys electricity

from the power grid, and the CHP system starts and stops twice a day. The photovoltaic output is small in the morning and evening, and at noon, when the photovoltaic output is large, the renewable energy is fully used. There are no power exchanges with the power grid.

The photovoltaic system outputs energy during the day. At the peak time, buying electricity from the grid is not economical. Therefore, it integrates photovoltaic systems into the charging stations, showing a good economy. The gas internal combustion engine in the CHP system is easy to start and stop, which could increase the power safety and stability of charging stations. According to the gas price and the safety and stability requirements of the charging station, it has more benefits with the appropriate gas generator sets. According to the above analysis, the mode of grid-connected and non-connected VPPs is adopted. For the charging station, a 10 MW photovoltaic system, 2 MW CHP unit, and 1 MW energy storage system are arranged to calculate the gas price. The price of the gas is 2 yuan/m³, and the charging cost of the electric vehicle is 1.4 yuan/kWh. The operation strategy is shown in traditional model in Figure 4. As shown in Figure 5, the energy storage station saves energy during the low electricity price at night and discharges during the daytime peak. In the case of the photovoltaic system, when the energy supply of the energy system is higher than the load demand, the energy storage increases the efficient operation of the energy system.

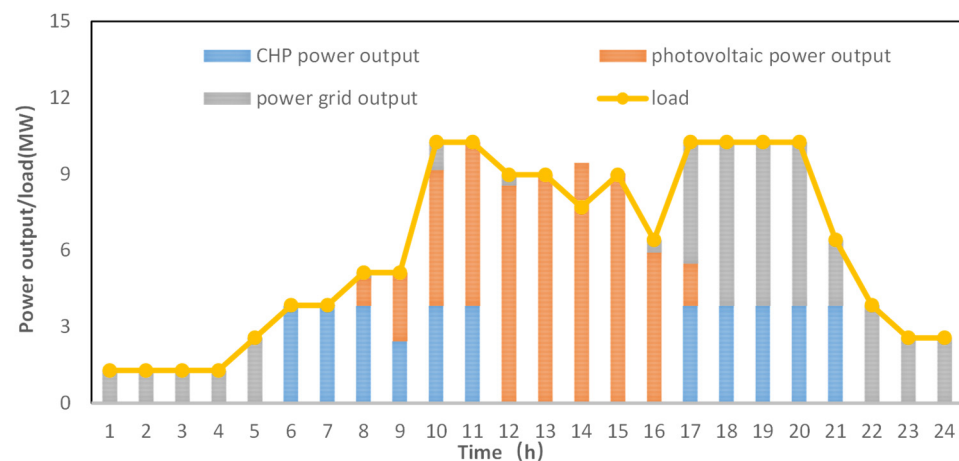


Figure 4. Power balance in traditional model without VPP.

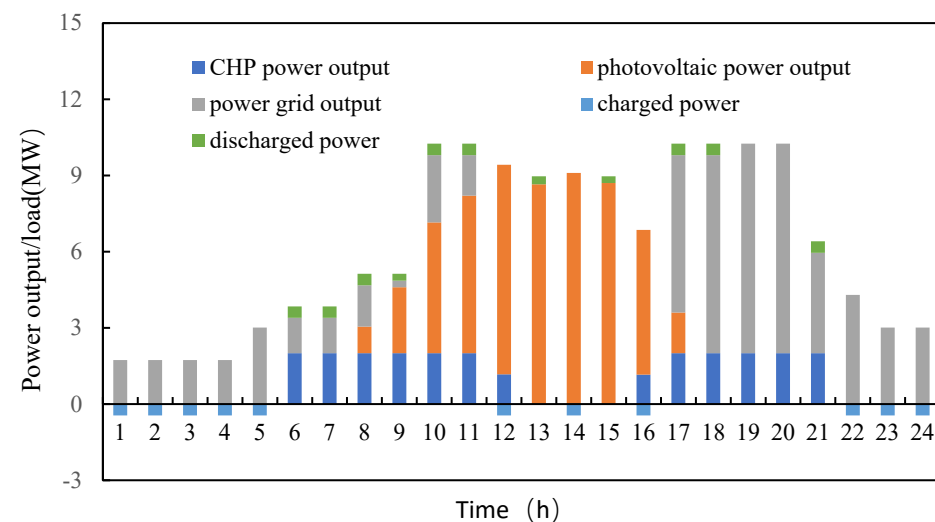


Figure 5. Power balance in the model with VPP.

According to the above, the VPP is modelled in Section 2. The typical daily operation situation is shown in Figure 6. Since all the power comes from the photovoltaic, CHP, and energy storage systems, the selected installed capacity must meet the real-time demand of the charging load. The equipment capacities are set relatively high, and the overall investment cost of the system is high. From the perspective of operation, the transmission power exceeds the demand in the low load period. The high output of renewable energy is greater than the load demand at noon. The energy storage system mainly stores renewable energy and releases electricity during the load peak period in the evening.

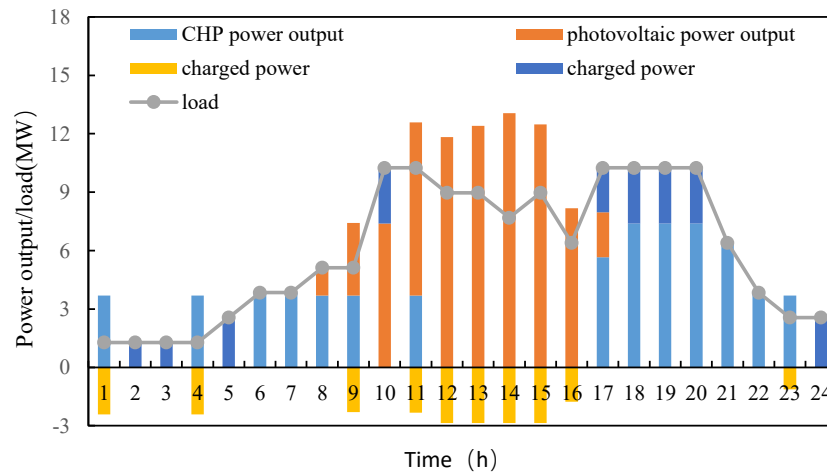


Figure 6. Power balance in the model with VPP and electric vehicle.

Figures 4–6 are the different scenarios of the traditional model, VPP model, and the VPP model with an electric vehicle. In Figure 4, there are no power exchanges with the power grid. The power exchanges with the power grid are shown in Figures 5 and 6. Moreover, the huge power exchanges are shown in Figure 6 which illustrates more profits for the VPP operator.

The orderly charging and discharging strategy are adopted in the VPP shown in Figure 7. The power interaction by electric vehicle load is changing, and the load distribution is more reasonable. Peak load filling is carried out, and no new load peak is generated which is conducive to keeping the safe operation of the power grid. The transformer has no overload. In the peak period of electricity consumption, the discharge is conducted by electric vehicle according to the demand of the users. It not only reduces the load rate of the transformer but also improves the income of the users.

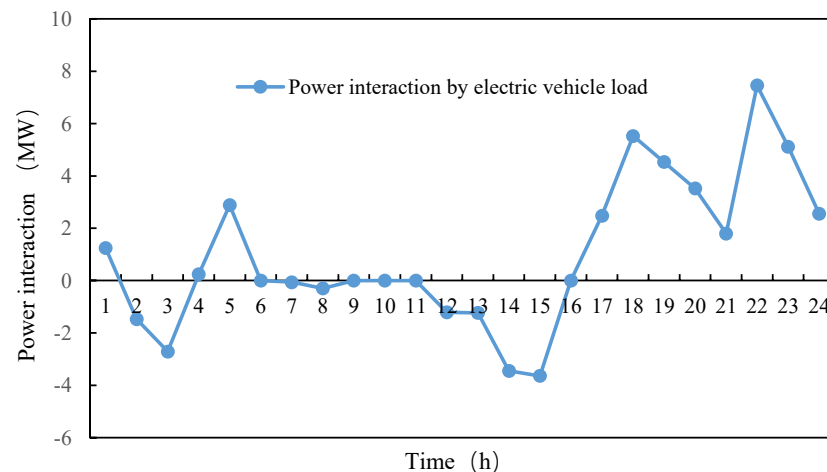


Figure 7. Power interaction between power grid and electric vehicle.

Figures 8 and 9 are the benefits of the proposed VPP model. We could give the conclusion that the charging price is the key point for the electric vehicle, which is the flexibility resources of the VPP. The CHP system has more income in the night when the power load is at its peak. Moreover, the flexibility resources based on the flexibility margin have more benefits all day.

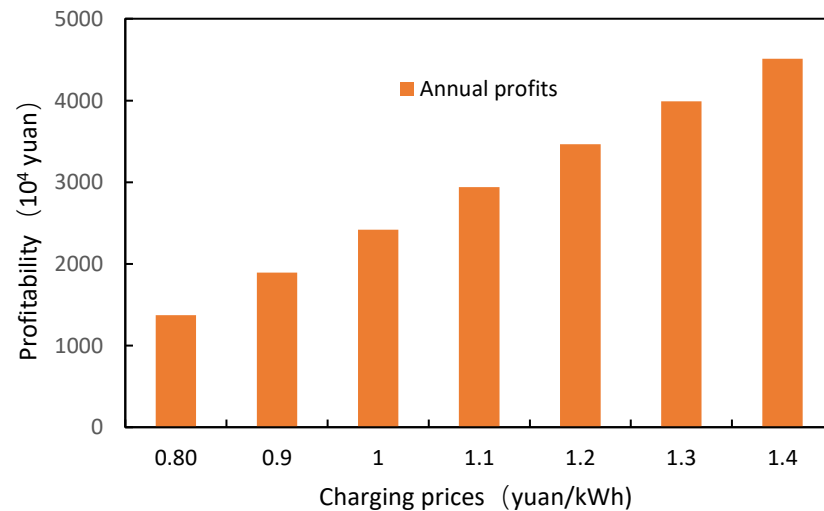


Figure 8. The annual profit of VPP with different charging prices.

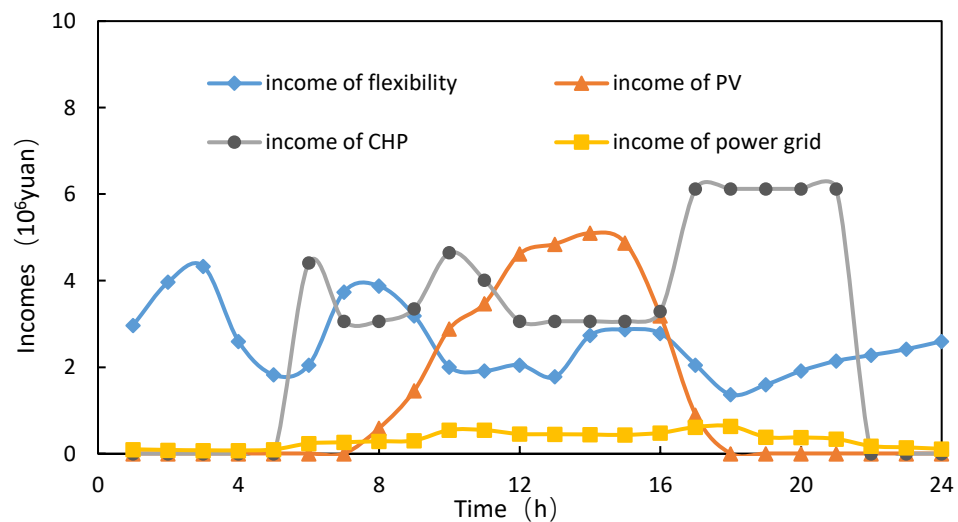


Figure 9. The incomes of different participants.

5. Conclusions

This paper puts forward the orderly charging and discharging strategy of electric vehicles in a VPP considering the needs and interests of users based on the flexibility margin in the VPP. The numerical results showed that the proposed VPP optimization method reduced the operation cost very well. The strategy could prevent overload, complete load transfer, realize peak shifting and valley filling, and solve the problems of peaks and new peaks caused by disorderly power utilization. Moreover, the VPP strategy proposed in this paper changes the multi-objective function into a single-objective function by optimizing the load model of electric vehicles which could increase the economic efficiency of the VPP. Finally, the orderly charging and discharging strategy of electric vehicles could reduce the charging cost for users participating in the peak-regulating auxiliary services market.

Author Contributions: Conceptualization, Y.T.; methodology, Y.Z.; validation, Z.L.; formal analysis, H.F.; investigation, J.W. and T.Z. All authors have read and agreed to the published version of the manuscript.

Funding: This work was supported by the National Natural Science Foundation of China (NSFC) (Grant No:51879140), State Key Laboratory of Hydrosience and Hydraulic Engineering (Grant No. 2021-KY-04), Tsinghua-Foshan Innovation Special Fund (TFISF) 2021THFS0209, and Creative Seed Fund of Shanxi Research Institute for Clean Energy, Tsinghua University.

Conflicts of Interest: The authors declare no conflict of interest.

Abbreviations

α_{PV}	the power temperature reduction coefficient in the standard state
η_E	the electric efficiency CHP
η_{EC}	the utilization efficiency of the electric refrigeration unit
η_{ES}	the self-discharge ratio
η_{ESC}	the charging efficiency
η_{ESD}	the discharge efficiency
η_H	the thermal efficiency CHP
η_{GB}	the gas utilization efficiency of the gas boiler
η_{loss}	the heat loss rate of CHP
η_{RC}	the refrigeration efficiency
$E_{ES\ min}$	the lower climbing limits (MW/h)
$E_{ES\ max}$	the upper climbing limits (MW/h)
$E_{ES}(t)$	The electric energy stored by the electric energy storage unit at time t (MW)
$E_{ES}(t - 1)$	the electric energy stored by the electric energy storage unit at time $t - 1$ (MW)
f_{pv}	the reduction coefficient
F_{GB}	the consumption of natural gas (m^3)
F_{GT}	the energy of gas combustion (MW)
F_{ru_up}	the upward flexibility margin (MW)
F_{ru_udown}	the downward flexibility margin (MW)
G	the illumination intensity of the current position (W/m^2)
G_S	the illumination intensity of the standard state (W/m^2)
P_C	the cooling load (MW)
P_E	the electric load (MW)
P_{EC}	the cooling output of the electric refrigeration unit (MW)
P_{EGT}	the electric power output by CHP (MW)
P_{ESC}	the charging power output (MW)
P_{ESD}	the discharge power output (MW)
$P_{ESC\ max}$	the rated charging power output (MW)
$P_{ESD\ max}$	the rated discharge power output (MW)
P_{grid}	the power supply of the power grid (MW)
P_{GB}	The thermal output power of the gas boiler (MW)
P_H	the thermal load (MW)
P_{HGT}	the thermal power output by CHP (MW)
P_{HRC}	the cooling output of the absorption refrigeration unit (MW)
P_{PV}	the power output of the photovoltaic power system (MW)
P_{PVR}	the rated power output in the standard state (MW)
P_{RC}	the cooling output and heating input of the absorption refrigeration unit (MW)
T	the temperature on the surface of the photovoltaic panel ($^{\circ}C$)
T_s	the temperature of the photovoltaic surface in the standard state ($^{\circ}C$)

References

1. Kong, X.; Xiao, J.; Wang, C.; Cui, K.; Jin, Q.; Kong, D. Bi-level multi-time scale scheduling method based on bidding for multi-operator virtual power plant. *Appl. Energy* **2019**, *249*, 178–189. [[CrossRef](#)]
2. Wei, C.; Xu, J.; Liao, S.; Sun, Y.; Jiang, Y.; Ke, D.; Zhang, Z.; Wang, J. A bi-level scheduling model for virtual power plants with aggregated thermostatically controlled loads and renewable energy. *Appl. Energy* **2018**, *224*, 659–670. [[CrossRef](#)]

3. Ju, L.; Tan, Z.; Yuan, J.; Tan, Q.; Li, H.; Dong, F. A bi-level stochastic scheduling optimization model for a virtual power plant connected to a wind–photovoltaic–energy storage system considering the uncertainty and demand response. *Appl. Energy* **2016**, *171*, 184–199. [[CrossRef](#)]
4. Riveros, J.Z.; Bruninx, K.; Poncelet, K.; D’haeseleer, W. Bidding strategies for virtual power plants considering CHPs and intermittent renewables. *Energy Convers. Manag.* **2015**, *103*, 408–418. [[CrossRef](#)]
5. Alsaleh, M.; Abdul-Rahim, A.S. Bioenergy industry and the growth of the energy sector in the EU-28 region: Evidence from panel cointegration analysis. *J. Renew. Sustain. Energy* **2018**, *10*, 53–61. [[CrossRef](#)]
6. Alsaleh, M.; Abdul-Rahim, A.S. Bioenergy Intensity and Its Determinants in European Continental Countries: Evidence Using GMM Estimation. *Resources* **2019**, *8*, 43. [[CrossRef](#)]
7. Royapoor, M.; Pazhoohesh, M.; Davison, P.J.; Patsios, C.; Walker, S. Building as a virtual power plant, magnitude and persistence of deferrable loads and human comfort implications. *Energy Build.* **2020**, *213*, 109794. [[CrossRef](#)]
8. Sikorski, T.; Jasiński, M.; Ropuszyńska-Surma, E.; Węglarz, M.; Kaczorowska, D.; Kostyla, P.; Leonowicz, Z.; Lis, R.; Rezmer, J.; Rojewski, W.; et al. A Case Study on Distributed Energy Resources and Energy-Storage Systems in a Virtual Power Plant Concept: Technical Aspects. *Energies* **2020**, *13*, 3086. [[CrossRef](#)]
9. Loßner, M.; Böttger, D.; Bruckner, T. Economic assessment of virtual power plants in the German energy market—A scenario-based and model-supported analysis. *Energy Econ.* **2017**, *62*, 125–138. [[CrossRef](#)]
10. Van Summeren, L.F.; Wieczorek, A.J.; Bombaerts, G.J.; Verbong, G.P. Community energy meets smart grids: Reviewing goals, structure, and roles in Virtual Power Plants in Ireland, Belgium and the Netherlands. *Energy Res. Soc. Sci.* **2020**, *63*, 101415. [[CrossRef](#)]
11. Ullah, Z.; Mokryani, G.; Campean, F.; Hu, Y.F. Comprehensive review of VPPs planning, operation and scheduling considering the uncertainties related to renewable energy sources. *IET Energy Syst. Integr.* **2019**, *1*, 147–157. [[CrossRef](#)]
12. Nosratabadi, S.M.; Hooshmand, R.-A.; Gholipour, E. A comprehensive review on microgrid and virtual power plant concepts employed for distributed energy resources scheduling in power systems. *Renew. Sustain. Energy Rev.* **2017**, *67*, 341–363. [[CrossRef](#)]
13. Arslan, O.; Karasan, O.E. Cost and emission impacts of virtual power plant formation in plug-in hybrid electric vehicle penetrated networks. *Energy* **2013**, *60*, 116–124. [[CrossRef](#)]
14. Ju, L.W.; Tan, Q.L.; Lu, Y.; Tan, Z.F.; Zhang, Y.X.; Tan, Q.K. A CVaR-robust-based multi-objective optimization model and three-stage solution algorithm for a virtual power plant considering uncertainties and carbon emission allowances. *Int. J. Electr. Power Energy Syst.* **2019**, *107*, 628–643. [[CrossRef](#)]
15. Cui, H.; Li, F.; Hu, Q.; Bai, L.; Fang, X. Day-ahead coordinated operation of utility-scale electricity and natural gas networks considering demand response based virtual power plants. *Appl. Energy* **2016**, *176*, 183–195. [[CrossRef](#)]
16. Kasaei, M.J.; Gandomkar, M.; Nikoukar, J. Optimal management of renewable energy sources by virtual power plant. *Renew. Energy* **2017**, *114*, 1180–1188. [[CrossRef](#)]
17. Luo, Z.; Hong, S.; Ding, Y. A data mining-driven incentive-based demand response scheme for a virtual power plant. *Appl. Energy* **2019**, *239*, 549–559. [[CrossRef](#)]
18. Li, Y.; Gao, W.; Ruan, Y. Feasibility of virtual power plants (VPPs) and its efficiency assessment through benefiting both the supply and demand sides in Chongming country, China. *Sustain. Cities Soc.* **2017**, *35*, 544–551. [[CrossRef](#)]
19. Alahyari, A.; Ehsan, M.; Mousavizadeh, M. A hybrid storage-wind virtual power plant (VPP) participation in the electricity markets: A self-scheduling optimization considering price, renewable generation, and electric vehicles uncertainties. *J. Energy Storage* **2019**, *25*, 100812. [[CrossRef](#)]
20. Sousa, T.; Morais, H.; Vale, Z.; Faria, P.; Soares, J. Intelligent Energy Resource Management Considering Vehicle-to-Grid: A Simulated Annealing Approach. *IEEE Trans. Smart Grid* **2012**, *3*, 535–542. [[CrossRef](#)]
21. Daraei, M.; Campana, P.E.; Thorin, E. Power-to-hydrogen storage integrated with rooftop photovoltaic systems and combined heat and power plants. *Appl. Energy* **2020**, *276*, 115499. [[CrossRef](#)]
22. Kolenc, M.; Nemček, P.; Gutsch, C.; Suljanović, N.; Zajc, M. Performance evaluation of a virtual power plant communication system providing ancillary services. *Electr. Power Syst. Res.* **2017**, *149*, 46–54. [[CrossRef](#)]
23. Bloess, A. Modeling of combined heat and power generation in the context of increasing renewable energy penetration. *Appl. Energy* **2020**, *267*, 1–17. [[CrossRef](#)]
24. Arteconi, A.; Mugnini, A.; Polonara, F. Energy flexible buildings: A methodology for rating the flexibility performance of buildings with electric heating and cooling systems. *Appl. Energy* **2019**, *251*, 113387. [[CrossRef](#)]
25. Magdy, F.E.Z.; Ibrahim, D.K.; Sabry, W. Energy management of virtual power plants dependent on electro-economical model. *Ain Shams Eng. J.* **2020**, *11*, 643–649. [[CrossRef](#)]
26. Yu, S.; Fang, F.; Liu, Y.; Liu, J. Uncertainties of virtual power plant: Problems and countermeasures. *Appl. Energy* **2019**, *239*, 454–470. [[CrossRef](#)]
27. Liu, Y.; Shen, Z.; Tang, X.; Lian, H.; Li, J.; Gong, J. Worst-case conditional value-at-risk based bidding strategy for wind-hydro hybrid systems under probability distribution uncertainties. *Appl. Energy* **2019**, *256*, 113918. [[CrossRef](#)]
28. Liang, Z.; Alsafasfeh, Q.; Jin, T.; Pourbabak, H.; Su, W. Risk-Constrained Optimal Energy Management for Virtual Power Plants Considering Correlated Demand Response. *IEEE Trans. Smart Grid* **2019**, *10*, 1577–1587. [[CrossRef](#)]
29. Adu-Kankam, K.O.; Camarinha-Matos, L.M. Towards collaborative Virtual Power Plants: Trends and convergence. *Sustain. Energy Grids Netw.* **2018**, *16*, 217–230. [[CrossRef](#)]

30. Robu, V.; Chalkiadakis, G.; Kota, R.; Rogers, A.; Jennings, N.R. Rewarding cooperative virtual power plant formation using scoring rules. *Energy* **2016**, *117*, 19–28. [[CrossRef](#)]
31. Guerrero, J.; Gebbran, D.; Mhanna, S.; Chapman, A.C.; Verbic, G. Towards a transactive energy system for integration of distributed energy resources: Home energy management, distributed optimal power flow, and peer-to-peer energy trading. *Renew. Sustain. Energy Rev.* **2020**, *132*, 110000. [[CrossRef](#)]
32. Hooshmand, R.A.; Nosratabadi, S.M.; Gholipour, E. Event-based scheduling of industrial technical virtual power plant considering wind and market prices stochastic behaviors—A case study in Iran. *J. Clean. Prod.* **2018**, *172*, 1748–1764. [[CrossRef](#)]
33. Obringer, R.; Mukherjee, S.; Nateghi, R. Evaluating the climate sensitivity of coupled electricity-natural gas demand using a multivariate framework. *Appl. Energy* **2020**, *262*, 114419. [[CrossRef](#)]
34. Shabanzadeh, M.; Sheikh-El-Eslami, M.-K.; Haghifam, M.-R. An interactive cooperation model for neighboring virtual power plants. *Appl. Energy* **2017**, *200*, 273–289. [[CrossRef](#)]

Disclaimer/Publisher’s Note: The statements, opinions and data contained in all publications are solely those of the individual author(s) and contributor(s) and not of MDPI and/or the editor(s). MDPI and/or the editor(s) disclaim responsibility for any injury to people or property resulting from any ideas, methods, instructions or products referred to in the content.